Chemical Engineering Journal xxx (xxxx) 135674

Contents lists available at ScienceDirect

Chemical Engineering Journal

journal homepage: www.elsevier.com/locate/cej

A bottom-up approach to generate isotropic liquid metal network in polymer-enabled 3D thermal management

Shen Chen [a, b], Wenkui Xing [a, b], Han Wang [a, b], Weizheng Cheng [a, b], Zhihui Lei [a, b], Feiyu Zheng [a, b], Peng Tao [a, b], Wen Shang [a, b], Benwei Fu [a, b], Chengyi Song [a, b, *], Michael D. Dickey [c, *], Tao Deng [a, b, *]

[a] The State Key Laboratory of Metal Matrix Composites, School of Materials Science and Engineering, Shanghai Jiao Tong University, 800 Dong Chuan Road, Shanghai 200240, PR China

[b] Center of Hydrogen Science, School of Materials Science and Engineering, Shanghai Jiao Tong University, 800 Dong Chuan Road, Shanghai 200240, PR China

[c] Department of Chemical and Biomolecular Engineering, North Carolina State University, 911 Partners Way, Raleigh, NC 27695, USA

ARTICLE INFO

Keywords:
Liquid metal
Bottom-up
Thermal conductivity
Isotropic Network
3D Thermal Management

ABSTRACT

This work presents a bottom-up approach to construct an isotropic network of liquid metal in polymer, and such generated isotropic liquid metal network brings large enhancement on the thermal and electrical conductivity of the composite for 3D thermal management. The building blocks are composed of polymer particles coated with liquid metal. The liquid metal starts to flow and fill the gaps between the polymer particles, and fuses with each other to assemble into a continuous liquid metal network in the polymer matrix under the mechanical load during heating. The continuous filler network provides effective paths for thermal and electrical conduction, and thus enhances the thermal and electrical conductivity of the composites. Using biphasic copper-eutectic gallium indium as the filler, we generated polymer composites with thermal conductivity as high as 32.71 W/m·K (90 vol%; under compression) and electrical conductivity up to 1.18×10^6 S/m. Moreover, the measurement of the in-plane and cross-plane thermal diffusivity reveals the isotropic enhancement of thermal conductivity in such composites, which may help expand the potential application of these composites in 3D thermal management, flexible electronics, energy conversion and soft robotics.

1. Introduction

Gallium-based liquid metals (Ga-based LMs) have shown interesting potential in different applications including thermal management, electronics and robotics due to the unique combination of rheological and metallic properties [1–6]. The challenge of potential leakage of LMs during operation, however, restricts their direct use as soft conductors in practical uses, especially for applications involving soft thermal conductors. In current research, LMs are usually used as fillers in a polymer matrix to minimize the leakage of LMs [7]. Compared to traditional rigid fillers, Ga-based LMs with their metallic thermal conductivity and their fluidic nature at room temperature possess good thermal conductivity enhancement of composites (TCE, i.e. $TCE = \frac{k_c - k_m}{k_m}$, where k_c and k_m are the thermal conductivity of the composite and polymer matrix, respectively) without degrading flexibility of the composite [8]. In most studies, LM inclusions in polymer matrix are achieved by mechanically mixing LM and uncured polymers [5,9]. For example, composites containing 50 vol% eutectic gallium indium (EGaIn) in silicone elastomer have thermal conductivity approaching ~ 1.5 W/m·K [2]. Nano-sized GaInSn droplets mixed with silicone oil can reach a volume fraction of 85.7% to produce a thermal conductivity of ~ 6.73 W/m·K [10]. The interfacial thermal resistance between LM inclusions and polymer matrix impedes effective heat transfer from one inclusion to another, and therefore represents an opportunity for greater enhancement [11,12].

Enabling thermal paths between different LM domains for heat conduction is an effective approach for further enhancing thermal conductivity [13,14]. Based on this strategy, two approaches have been explored. Stretching is one of the effective approaches to enhance the thermal conductivity of polymer-based composite with LM fillers. The thermal conductivity in the stretching direction can be greatly enhanced due to the orientation of the internal elongated LM inclusions and the formation of the thermal path along the stretching direction. A thermal conductivity up to 9.8 W/m·K along the stretching direction was reported with a strain of 400% for 50 vol% EGaIn/silicone elastomer composite, but the thermal conductivity would drop to 4.9 W/m·K along the stretching direction after removing the drawing load [2].

* Corresponding authors.
E-mail addresses: chengyi2013@sjtu.edu.cn (C. Song), mddickey@ncsu.edu (M.D. Dickey), dengtao@sjtu.edu.cn (T. Deng).

https://doi.org/10.1016/j.cej.2022.135674
Received 18 January 2022; Received in revised form 20 February 2022; Accepted 5 March 2022
1385-8947/

To overcome such challenge, the authors further annealed the stretched EGaIn/polymer composite to fix the elongated LM inclusions [15]. After annealing, in-plane thermal conductivity as high as 13 W/m·K could be obtained in 70 vol% EGaIn/polymer with a strain of 200%. Though the in-plane thermal conductivity is high, the low cross-plane thermal conductivity still limits the potential space of such composites. In addition to stretching, building 3D network provides effective thermal paths for heat conduction to enhance the overall thermal conductivity [16]. The filler network formation in the polymer matrix have been reported in recent years, such as graphene platelets network, expanded graphite network and so on, with its effect on the improvement of thermal properties explored [17–19]. A LM foam based on vacuum-assisted infiltration in sacrificial sugar templates generated a composite by backfilling silicozzne prepolymer [20]. With a volume fraction of 25%, the thermal conductivity was ~ 2.7 W/m·K. Such vacuum-assisted infiltration approach, however, is challenging for highly viscous LM-based fillers, such as pastes containing EGaIn and solid fillers (i.e. Cu or Ag). A more versatile approach that can construct 3D LM thermal paths with a wide range of LM-based fillers is thus needed.

Here, we reported a simple, alternative approach to generate polymer-based composites with isotropic TCE in 3D by taking advantage of the fluidity of LM-based fillers through mechanical load under heating. Procedures involving mechanical load under heating have been used for the fabrication of polymer composites with enhanced thermal conductivity [16]. However, most of these previous efforts used polymer microspheres covered with solid 2D fillers, including graphene and BN nanosheets, and the composites tended to show the enhancement of thermal conductivity in the in-plane direction, which may also limit the range of practical applications [21–24]. In this work, different from traditional methods of producing metallic network based on foaming and templating [25–27], we adopted a bottom-up approach for the generation of LM network in thermoplastic elastomer (TPE) by applying mechanical load to TPE particles coated with LM during heating (Fig. 1). The applied mechanical load during heating helps the LM-based inclusions flow and fill the gaps between the TPE powders, and assemble into an isotropic LM network.

To demonstrate the applicability of this strategy for various LM-based fillers of different viscosity, we studied two typical LM-based fillers pure gallium (Ga, with a low water-like viscosity) and a biphasic paste containing silane molecules modified spherical Cu particles in EGaIn (CuP-EGaIn, relatively high viscosity). At the same volume fraction, the thermal conductivity of the Ga network/TPE composite (GN/TPE, e.g. ~ 50 vol% GN/TPE, 3.29 W/m·K) is more than twice of the thermal conductivity of the composites fabricated by directly mixing (50 vol% EGaIn/PDMS, ~1.5 W/m·K [2]). Such enhancement is attributed to the formation of 3D network of thermally conductive Ga. Remarkably, we also studied the influence of the size of TPE particles on the thermal conductivity of composites and found that composites prepared by larger TPE particles showed higher thermal conductivities, which enabled tunable thermal conductivities by changing the size of TPE particles. For a composite of 90 vol% CuP-EGaIn network/TPE with polymer particle size of 400 μm (90 vol% CGIN/TPE-400μ m), the thermal conductivity is as high as 32.71 W/m·K in both in-plane and cross-plane directions, which is among the highest values achieved in all polymer-based composites using LM-based fillers. The results of mechanical test demonstrated compressible and stretchable characteristics of the composites, which is important in real uses. Moreover, the network is electrically conductive in 3D. The electrical conductivity of the 50 vol% GN/TPE composites (2.13×10^5 S/m) is one order of magnitude higher than that of the 50 vol% GaInSn/PDMS composite (1.05×10^4 S/m), which was generated through mechanical sintering of LM droplets in silicone[9]. The electrical conductivity of the 90 vol% CGIN/TPE composite is ~ 1.18×10^6 S/m, which is close to the electrical conductivity of pure EGaIn (3.4×10^6 S/m. At last, we tested the heat dissipation performances of our composites and the results of both in-plane and cross-plane heat dissipation were superior to commercial thermal pads. This work provides a facile and versatile approach for the fabrication of high performance thermal interface materials (TIMs), and also offers a new insight in designing tailorable filler network based on the fluidity of fillers in enhancing thermal and electrical conductivity in 3D for a wide range of applications, including thermal management, flexible electronics, energy conversion and soft robotics [29].

2. Materials and methods

2.1. Materials

Gallium-based liquid metals including gallium and EGaIn alloy, purchased from Jiachun Commercial Bank, Fushun, Liaoning, China, are used as high-κ inclusions. Thermoplastic elastomer (TPE, 500 mesh, melting point ca. 120°C) powders, provided by Suzhan Plastic, Dongguan, Guangdong, China, are used as polymer matrix and dried in air at 60 °C for 3 h before the use. Spherical Cu particles (the size is ~ 40 μm), purchased from Tuopu Metal Materials Co., Ltd, Xingtai, Hebei, China, are used as fillers in TPE and also added into EGaIn to obtain a paste-like CuP-EGaIn with higher thermal conductivity.

2.2. Methods

2.2.1. Fabrication of GN/TPE composites

Probe ultrasonication was used to disperse bulk gallium into microdroplets in ethanol for 10 min with a power of 120 W [30,31]. The gallium microdroplets solution was then poured into TPE powders and mixed uniformly until the slurry showed a uniform color. After drying at room temperature overnight until all the residue solvent was vaporized, uniform mixture of powders of Ga and TPE were obtained. After grinding the dried mixture, the mixture powders were placed in a homemade PTFE mold followed by applying a mechanical pressure of 1 MPa at 135 °C for 15 min to obtain the GN/TPE composite.

2.2.2. ***Fabrication of CGIN/TPE composites*** [32]

20 g of spherical Cu particles was sonicated in ethanol and cleaned for 0.5 h. The cleaned Cu particles were then immersed in toluene solution with 16.7 mmol 3-Chloropropyltriethoxysilane (CPTES) and stirred for 24 h by an electric mixer at a rate of 600 rpm. The modified Cu particles were rinsed with ethanol for three times and then dried in a 60 °C oven. 10g of modified Cu particles were added into 5g of liquid EGaIn metal. We mixed them uniformly using a mortar and a pestle to prepare the composite of CuPs and EGaIn (CuP-EGaIn), which was used as highly viscous liquid metal-based fillers in this work. The paste-like liquid metal composite was directly mixed with TPE powders using a mortar and pestle to get them uniformly mixed. Such mixture was then placed in the PTFE mold under 1 MPa at 135°C for 15 min to obtain the CGIN/TPE composite.

2.2.3. Fabrication of CuP/TPE composites

Spherical Cu particles were mixed with TPE powders using a mortar and pestle to obtain the uniformly mixed powders. Followed by the same process with mechanical load under heating, CuP/TPE composites could be obtained.

2.2.4. Characterization

The morphology and the phase distribution in the composite were observed by the Scanning Electron Microscope (SEM, */TESCAN MAIA3 GMU model 2016/WITec apyron) and the elemental distribution in the composites was characterized by the Energy Dispersive X-ray Spectroscopy Probe in the SEM. X-ray microscope (micro-CT, Xradia 520 Versa) was used to reconstruct the 3D microstructure of the composites. The electrical conductivity was tested by a customized four-probe method using Keithley 2450 source measuring unit. TIM Thermal Resis-

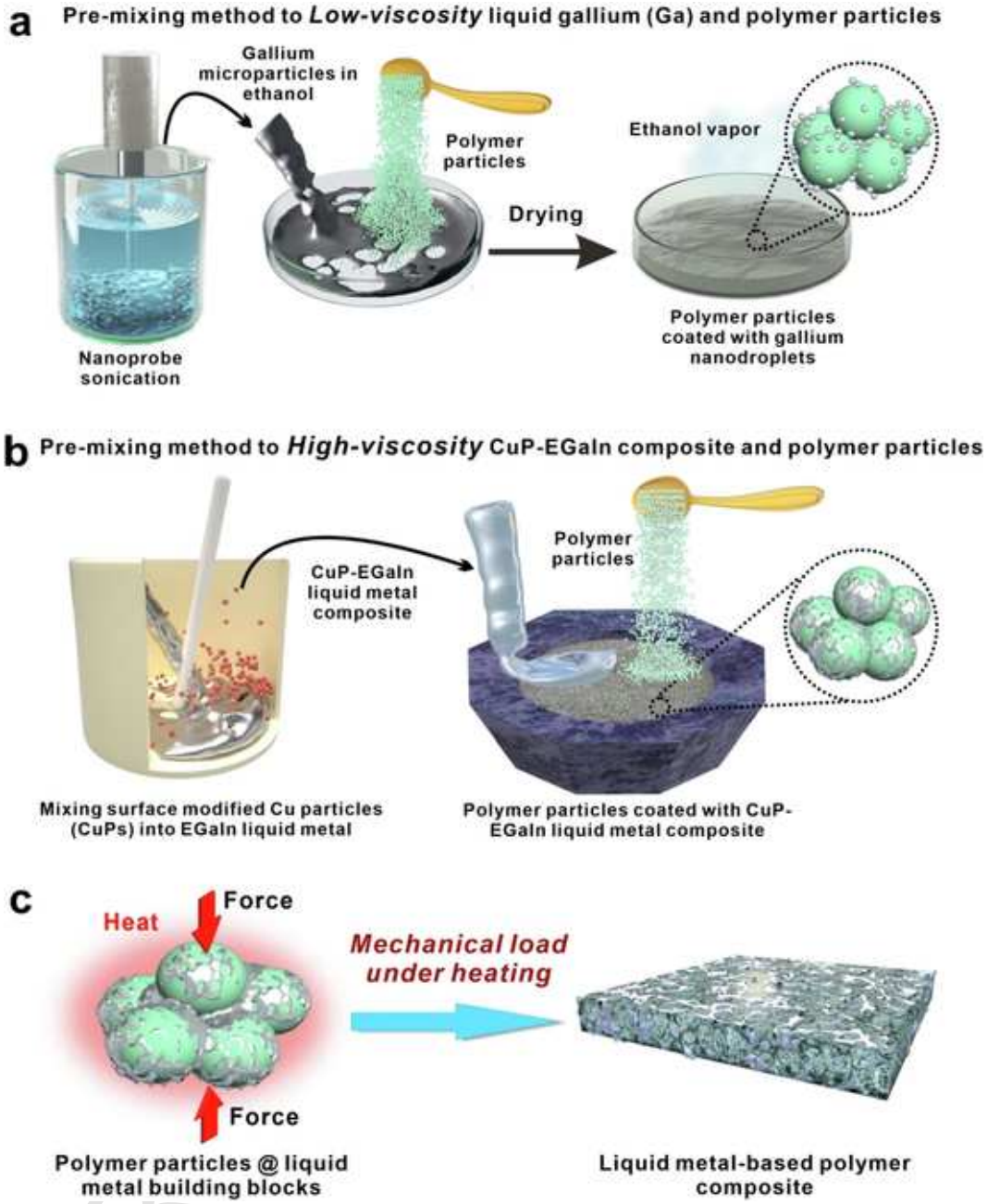

Fig. 1. The schematic of the fabricating procedure of low-viscosity liquid gallium/polymer particles (a) and high-viscosity semi-liquid CuP-EGaIn composite/polymer particles (b). (c) Schematic illustration of preparation of isotropically thermal and electrical conductive LM-based polymer composite via mechanical load under heating.

tance and Conductivity Measurement Apparatus (LW-9389, Taiwan Long Win Science and Techonology Co.) was employed to measure the thermal conductivity of the composites. The thermal diffusivity was measured by a laser flash diffusivity instrument LFA 467 (NETZSCH, Germany). The impact test was observed with a high-speed camera (AOS Technologies AG, S-VIT LS). The infrared (IR) images of LED were visualized by an IR camera (FLIR T620).

3. Results and discussion

3.1. Morphology and structure of the GN/TPE polymer composite

Thermoplastic elastomer (TPE) is appealing because it is elastomeric, yet can flows at elevated temperatures. The thermoplastic segments of the copolymer form physical crosslinks and the rubber segments contribute to elasticity. In previous efforts for the generation of polymer composites, polymer powders and solid fillers, such as BN, graphene and hybrid fillers, get mixed prior to the application of mechanical load under heating [16,21–24]. In this work, the direct mixing approach is not applicable due to the high surface tension and low viscosity of Ga [1,33]. As shown in **Figure S1(a)**, there were still bulk Ga droplets that could not be blended with TPE powders even after prolonged direct mixing. To overcome this challenge, we first broke the bulk Ga droplets into Ga microdroplets using ultrasonication. After ~ 10-min probe ultrasonication, bulk Ga was dispersed into ethanol as spherical microdroplets with the size ranging from 1 to 2 μm (**Figure S2(a)**) [30,31]. TPE powders were then mixed with the ethanol solution of Ga microdroplets until the mixture slurry showed a uniform color. After drying, the powder mixtures appeared grey. As shown from the scanning electron microscopy (SEM) image of the dried powder

mixture in Fig. 2**(a)** and Fig. 2**(b)**, Ga microdroplets densely covered the surface of TPE particles due to the capillary force generated during the evaporation of ethanol. Ga microdroplets will undergo sintering under the external load (**Figure S2**) and then cover the surface of TPE particles. It was reported that the formation of gallium oxide in oxygen-rich environments could allow highly nonwetting particles to be dispersed into LM [33]. During the mixing process of gallium-based LM, gallium oxide thin films could be easily formed when the fresh LMs were exposed to air. The generated oxide films could help encapsulate TPE particles into gallium-based LMs [32]. Such TPE particles with a coating of Ga microdroplets serve as the basic building blocks for the bottom-up formation of the network of Ga in the subsequent step of mechanical load under heating (Fig. 1).

In the mixture, Ga remains fluidic, so the Ga microdroplets can readily flow and fill the gaps between TPE powders to form the 3D network under both the mechanical load and heating. Meanwhile, TPE particles melt and then merge into continuous 3D network in the composite. Phase segregation is clearly seen in Fig. 2**(c(i))**, where grey areas are TPE and dark areas are Ga. Both the zones of TPE and Ga show irregular shape owing to the fluid nature of both Ga and TPE during the mechanical load under heating. In particular, the fluid nature of Ga plays a critical role in the formation of the continuous structure of Ga network, which acts as a thermal highway for heat conduction. In previous efforts that involved the mechanical load under heating, most of them used solid fillers [21–24]. To promote the interconnection of such solid fillers to form a continuous network, it required modifying the surface chemistry of polymer microspheres or fillers [21,34]. The fluid nature, however, endows Ga the ability to flow and fill the gaps among TPE particles without need of surface modification of particles of polymer matrix.

To further visualize the distribution of Ga and TPE, energy dispersive spectroscopy (EDS) mapping characterized the cross section of the GN/TPE composite. Fig. 2**(c(ii)-(iv))** show the continuous nature of the network structure of Ga. Such a continuous network of Ga greatly enhances the overall thermal conductivity in 3D for providing an effective path for heat conduction as well as electrical conduction. Fig. 2**(d)** shows the reconstructed 3D microstructure of the GN/TPE composite characterized by micro-computed tomography (Micro-CT). The light-yellow zones consist of Ga, which forms a network structure in 3D. The uniform distribution of the network shown in both the vertical and the horizontal cross-section images indicates a 3D network, which can facilitate the thermal and electrical transport in both the in-plane and cross-plane directions of the composites. The GN/TPE composites are flexible because of the elastomer matrix and fluid nature of Ga. Fig. 2**(e)** shows that the sample is bendable and could be folded in half without any cracks. The flexibility and deformability will be helpful for its potential application as TIMs.

3.2. Thermal/electrical performance of GN/TPE polymer composite and finite element analysis on the thermal conduction

Fig. 3**(a)** shows the schematic diagram of the setup for the measurement of thermal conductivity (LW-9389, TIM Thermal Resistance and Conductivity Measurement Apparatus, Taiwan Long Win Science and Technology Co.). We also fabricated Cu particle/TPE (CuP/TPE) composites by directly applying load to the mixture of spherical Cu particles and TPE particles during heating to provide a control group. The SEM and optical images of Cu particles are shown in **Figure S3**. Fig. 3**(b)** compares the thermal conductivity of the GN/TPE composites and CuP/TPE composites under different volume fractions of filler. The thermal conductivity of the pure TPE is 0.22 W/m·K. As the volume fraction of metallic filler increases, the thermal conductivity of both composites increases. The thermal conductivity of GN/TPE, however, increases much more than that of CuP/TPE with respect to filler loading. When the volume fraction of Ga reaches 50%, the thermal conductivity of GN/TPE is ~ 3.29 W/m·K, with nearly 14-fold TCE over the original TPE. With the same volume fraction of filler, the thermal conductivity of GN/TPE is more than twice as much as that of CuP/TPE. Considering the thermal conductivity of Cu is 397 W/m·K, much higher than that of Ga (29 W/m·K), such enhancement is attributed to the different filler distribution as is shown in Fig. 2**(c)** and **Figure S4(a)**. The continuous Ga network in the GN/TPE composites can provide effective thermal paths for heat conduction, while dispersed Cu particles in the CuP/TPE composites cannot.

The thermal performance of GN/TPE and CuP/TPE composites can be simulated by Agari s model, which is a classic model for considering

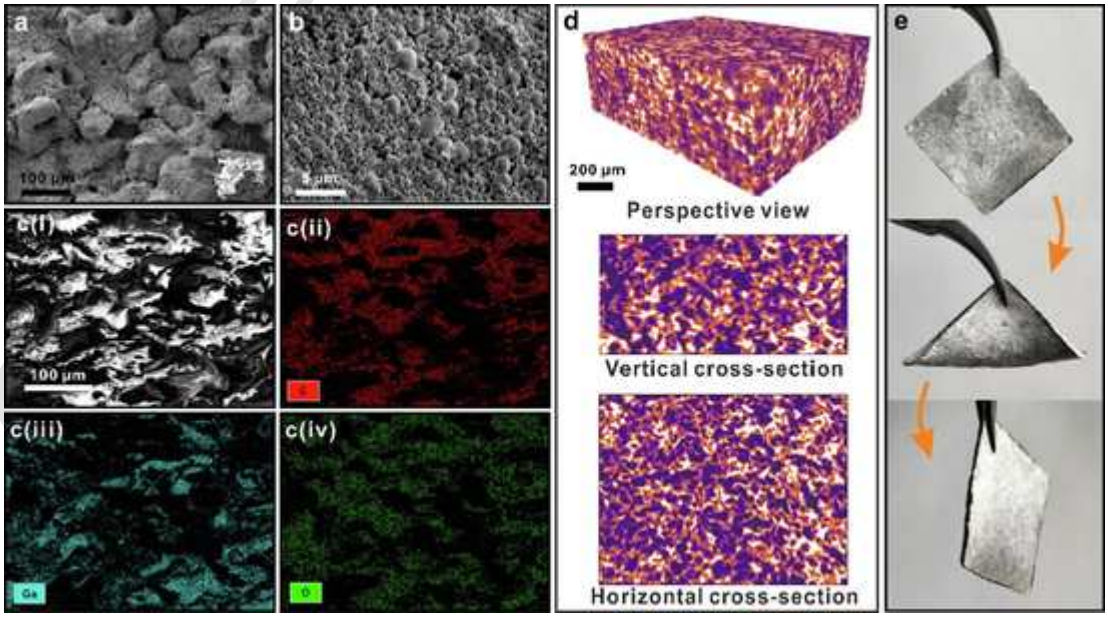

Fig. 2. (a) 30 vol% GN/TPE mixture powders after drying; (b) The magnified surface morphology of 30 vol% GN/TPE mixture powders after drying; (c-i) The SEM images of 32.7 vol% GN/TPE composite after mechanical load under heating, and the energy dispersive spectroscopy (EDS) of (c-ii) carbon, (c-iii) gallium and (c-iv) oxygen in 32.7 vol% GN/TPE composite; (d) 3D microstructure of the GN/TPE composite reconstructed by micro-computed tomography (Micro-CT); (e) The optical images of 30 vol% GN/TPE composite and the states in bending and after bending.

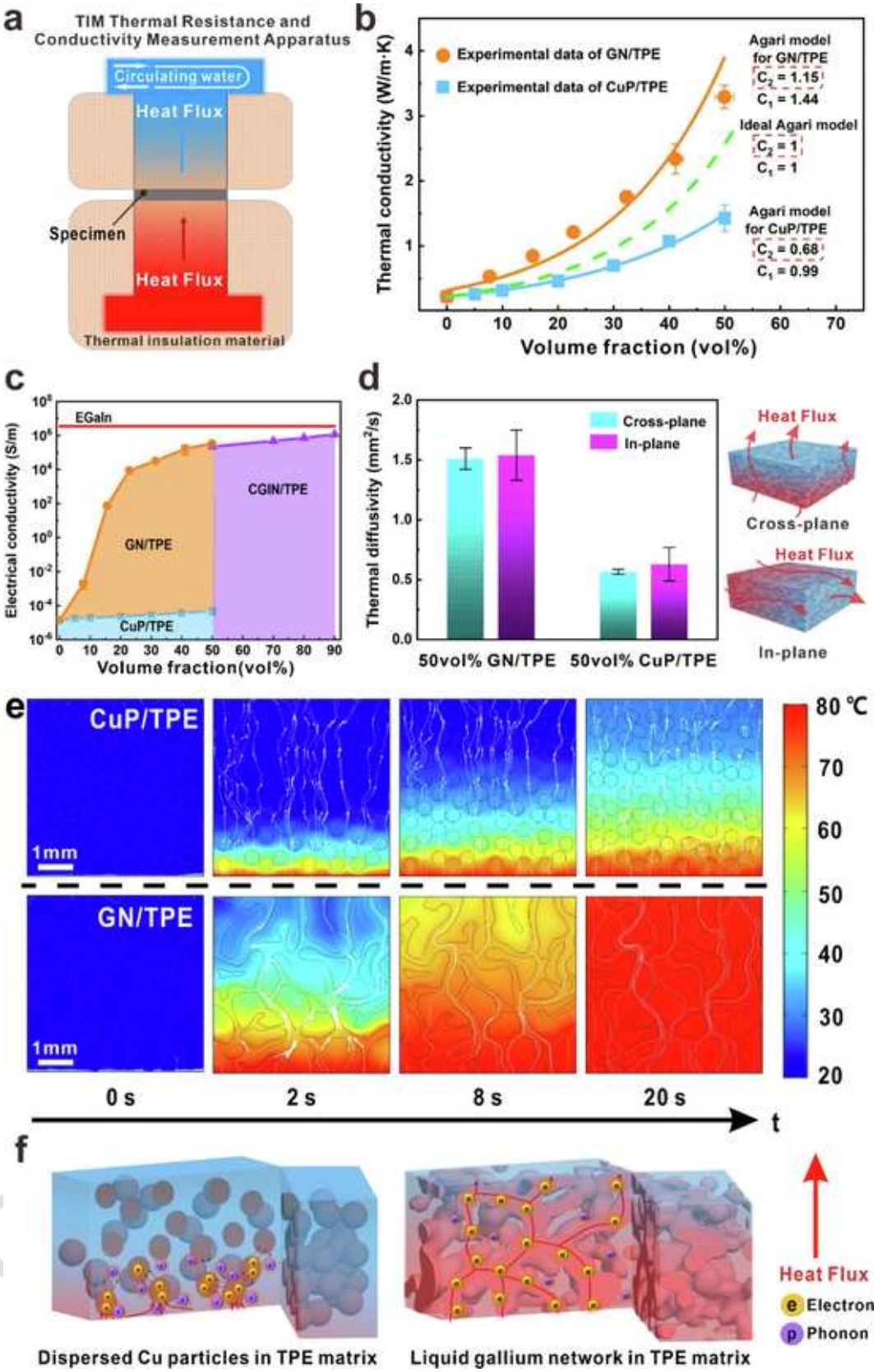

Fig. 3. (a) Schematic of thermal interface materials (TIM) measurement apparatus; (b) The thermal conductivity of Ga network/thermoplastic elastomer (GN/TPE) composites and Cu particles/TPE (CuP/TPE) composites with different volume fraction of filler; (c) The electrical conductivity of GN/TPE, CuP/TPE and CuP-EGaIn network/TPE (CGIN/TPE) composites with different volume fractions of filler; (d) The in-plane and cross-plane thermal diffusivities of 50 vol% GN/TPE and 50 vol% CuP/TPE composites; (e) Finite element analysis on the thermal conduction by COMSOL Multiphysics 5.4. The evolution of temperature in CuP/TPE composites and

◀ GN/TPE composites. The white streamlines and arrows represent heat flux and the direction of the heat flux, respectively; (f) Schematic mechanism of thermal conduction in CuP/TPE composites and GN/TPE composites, respectively.

the effect of fillers on the thermal conductivity [35–38]. The thermal conductivity of the composite (k_c) can be predicted based on the following **Eq. (1)**:

$$\log k_c = V_f \cdot C_2 \cdot \log k_f + (1 - V_f) \cdot \log(C_1 \cdot k_p) \quad (1)$$

where k_f and k_p are the thermal conductivities of fillers and polymer matrix, respectively. V_f is the volume fraction of fillers. C_1 represents the effect of fillers on the change in crystallinity and crystal size of polymer matrix. C_2 indicates the ease of fillers to form thermal conductive paths, and its value should be between 0 and 1. As the possibility to form thermal conductive paths increases for the fillers, there will be increased contribution to the overall thermal conductivity of the composite from the fillers, and C_2 approaches to 1 [37]. By using the Agari s model to fit the experimental data of the GN/TPE and CuP/TPE composites in Fig. 3**(b)**, the calculated C_2 is 1.15 and 0.68, respectively. In Agari s model, the highest thermal conductivity is predicted when both C_1 and C_2 are set as 1. The prediction is plotted in Fig. 3**(b)**. We observed that the ideal Agari s values for GN/TPE (green dash line) are higher than those of the CuP/TPE composites as expected but lower than the experimental results of the GN/TPE composites. We concluded that the LM network provides more effective thermal transfer paths than solid fillers can offer, since the Agari s model is empirically established for dispersed solid fillers. Such a result reflects that the formation of continuous filler network is much more effective and efficient than the dispersed fillers in enhancing thermal conductivity. To visualize the difference, heat transfer behavior of the two kinds of filler system (dispersed fillers and continuous 3D filler network) will be simulated via finite element analysis.

The electrical conductivity also reveals the different spatial distribution of fillers in the GN/TPE and CuP/TPE composites. Fig. 3**(c)** is the dependence of electrical conductivity of the composites on the filler content. With the increase of Ga content, Ga inclusions gradually connect with each other to form networks. The electrical conductivity rises rapidly with the formation of the metallic network. When the volume fraction of Ga is up to 50%, the electrical conductivity of the composite is up to 2.13×10^5 S/m. The variance in electrical conductivity is negligible in the range from 0 to 50 vol% for CuP/TPE composites. In CuP/TPE composites, there is no electrical conductive path for the current due to the isolated Cu particles surrounded by the insulated TPE, as shown in **Figure S4**.

Laser flash analysis (LFA) was used to characterize the thermal diffusivities of GN/TPE and CuP/TPE composites along both of the in-plane and cross-plane directions (**Figure S5**). As the specific heat and density of the same sample are constant, the thermal diffusivity in the in-plane and cross-plane directions will show whether the thermal conductivity of a sample is isotropic or not. Fig. 3**(d)** shows that the in-plane and cross-plane thermal diffusivities of 50 vol% GN/TPE are 1.609 and 1.569 mm^2/s. For the CuP/TPE composites, the in-plane and cross-plane diffusivities are also similar (Fig. 3**(d)**). These measurements show that this process can achieve high thermal conductivity in both of the in-plane and cross-plane direction at the same time, which will enhance the applicability of the LM-based composites.

To further demonstrate the impact from the dispersed fillers and the continuous filler network on the thermal conductivity of the composites, finite element analysis by COMSOL Multiphysics 5.4 was used to simulate the thermal conduction behavior. The 2D models of pure TPE, CuP/TPE and GN/TPE composites were established for the analysis. Details of the models and the parameters (Table S1) of the simulation can be found in the supporting information. Transient-state studies were adopted to compare the evolution of temperature within the composites. The temperature of bottom boundaries was fixed to 80°C and the top boundaries had a convection coefficient of 10 W/m^2K in a 20°C ambient, with two sides set as adiabatic boundaries. **Figure S6** and Fig. 3 **(e)** show the evolution of the temperature distribution and heat flux within the modeled pure TPE, CuP/TPE and GN/TPE composites. According to the temperature distribution in Fig. 3**(e)**, it is clear that heat transfers from bottom sides to top sides much faster in GN/TPE than in pure TPE and CuP/TPE, which indicates the large difference in thermal conductivity of the three composites. After 20 s, the temperature of the top boundaries reaches 22.16 °C, 30.78 °C and 77.65 °C for the pure TPE, CuP/TPE and GN/TPE composites, respectively. White streamlines and arrows in the models represent the distribution and direction of heat flux. Heat fluxes distribute uniformly in pure TPE, while they tend to converge on the Cu particles in the CuP/TPE composite. The convergence of heat fluxes in the GN/TPE composite is much more obvious, and almost all heat streamlines concentrate in the region of Ga network, which implies heat flux preferentially transfers in regions with high thermal conductivity. Such results reveal the difference of thermal conduction behavior in the three different composites, and help corroborate the aforementioned mechanism that the formation of filler network can greatly enhance the thermal conductivity of the composites.

Steady-state studies were also carried out for predicting the thermal conductivity of the composites and detailed information is presented in supporting information. To satisfy the practical condition, we accounted for interfacial thermal resistance in the simulation and supposed that the gap thermal conductance between the filler and polymer matrix is 5×10^7 W/m^2K [39]. The prediction of thermal conductivity is based on the Fourier's law **(Eq. (2))**:

$$k = \frac{q}{dT/dx} \quad (2)$$

where k is the thermal conductivity; q is the heat flux and dT/dx represents the temperature gradient in the direction of heat flux when the system reaches steady state. The average values of predicted thermal conductivities of 50 vol% CuP/TPE and 50 vol% GN/TPE are 1.18 and 3.39 W/m·K, respectively. These values are consistent with the trend showing in the experimental results (1.43 and 3.29 W/m·K for 50 vol% CuP/TPE and 50 vol% GN/TPE, respectively) (**Figure S7** and Table S2). It also confirms that both the increasing volume fraction and the improvement of intrinsic thermal conductivity of filler network help further increase the overall thermal conductivity of the composites.

Fig. 3**(f)** depicts the difference of thermal conduction behavior in the CuP/TPE and GN/TPE composites, respectively. In the CuP/TPE, Cu particles are dispersed in isolation and encased by polymer matrix. The electron transportation in Cu particles is blocked by the insulating polymer matrix, and strong phonon scattering occurs at the interface between the Cu particles and polymers, both of which result in the relatively low thermal conductivity of the CuP/TPE composites. In contrast, the continuous network of GN/TPE provides effective propagation paths for heat carriers that include both electrons and phonons. The heat carriers can readily transfer along the channels of the Ga network from the hot side of the composite to the cold side of the composite.

3.3. Morphology and physical properties of the CGIN/TPE polymer composites

As for high-viscosity liquid metal, for example, CuP-EGaIn liquid metal composites [28], can be more easily blended with TPE powder particles through the direct mixing approach. In the next experiment, we generated the high-viscosity liquid metal 3D network in TPE polymer matrix with CuP-EGaIn, which is a biphasic and high-viscosity paste containing Cu particles in EGaIn. The preparation of CuP-EGaIn network/TPE (CGIN/TPE) composite is straightforward. In our recent

published work, we have developed a new approach to fabricate Cu particles and EGaIn liquid metal composite with enhanced thermal conductivity and chemical stability [32]. Spherical Cu micro-particles chemically modified with 3-chloropropyltriethoxysilane (CPTES) molecules were incorporated into liquid EGaIn with the assistance of air. The formation of intermetallic compounds $CuGa_2$ can be largely suppressed, but the overall thermal conductivity of liquid metal composite can be still enhanced through thermal linker CPTES molecules [32] (see the detailed fabrication process in Method section) (Fig. 4**(a)**). With the high viscosity and good adhesion to the TPE powder, paste-like CuP-EGaIn could be easily mixed with TPE powders to obtain the uniform mixture of powders (**Figure S1(b)**). To show the increased viscosity of CuP-EGaIn over the pure Ga LM, we conducted a simple impact test (**Figure S8**). Dropped from the same height of 0.5 m, the spreading area of the Ga droplet was much larger than that of CuP-EGaIn, which indicated the liquid-like behavior of Ga and paste-like behavior of CuP-EGaIn.

Though CuP-EGaIn paste shows high viscosity, it still has the capability to flow and fill the gaps during the mechanical load under heating to form a continuous 3D network embedded in TPE matrix. The continuous distribution of CuP-EGaIn is clearly seen in **Figure (4b(i)(ii))** and spherical Cu particles are embedded in the EGaIn network as shown in the image of EDS mapping in Fig. 4**(b(ii))**. The dispersed Cu particles in EGaIn can further enhance the thermal conductivity of the network [28, 32]. Compared to the case in CuP/TPE composites (**Figure S4**), EGaIn acts as a glue to connect Cu particles instead of being isolated throughout the bulk composite. For 80 vol% CGIN/TPE, the average values of in-plane and cross-plane thermal diffusivities shown in **Figure S9** are 7.39 and 7.09 mm^2/s, respectively. The similar values between the in-plane and cross-plane thermal diffusivities reflect the isotropic structure of the network in the composites, as the same with that in GN/TPE composites (Fig. 2**(c)**). Fig. 4**(c) and (d)** display the soft feature of the CGIN/TPE composites. The CGIN/TPE composites with filler of different volume fractions are bendable and stretchable to some extent, which indicates the applicability of the composites in thermal management applications.

Considering the soft properties of CGIN/TPE composites, we measured the thermal conductivity under the compression (with the pressure of 100 Psi). As shown in Fig. 4**(e)**, with different volume fractions, the thermal conductivities measured under compression are always higher. The thermal conductivity is 20.11 W/m·K before compression and then increases to 24.40 W/m·K during the compression, when we incorporated 90 vol% CuP-EGaIn into the composite. It was studied that the elastomer would return to its original state slowly without external pressure [2,40]. The TPE elastomer in the composites may undergo springback slightly after the mechanical load and heating. When the sample was measured under the compression, the composite was compressed to be denser and the interconnection of filler become more complete. Therefore, the interface thermal resistance inside the sample were reduced under the compression, leading to the enhancement of overall thermal conductivity. The stretching properties are displayed by the typical stress–strain plots shown in Fig. 4**(f),** which indicate characteristics of plasticity and ductileness. From the stress–strain plots, we calculated the breaking strain and breaking strength, and the results are shown in Table S3. We did not give the stretching result of the 90 vol% CGIN/TPE composite since it is fragile and cannot be clamped in the

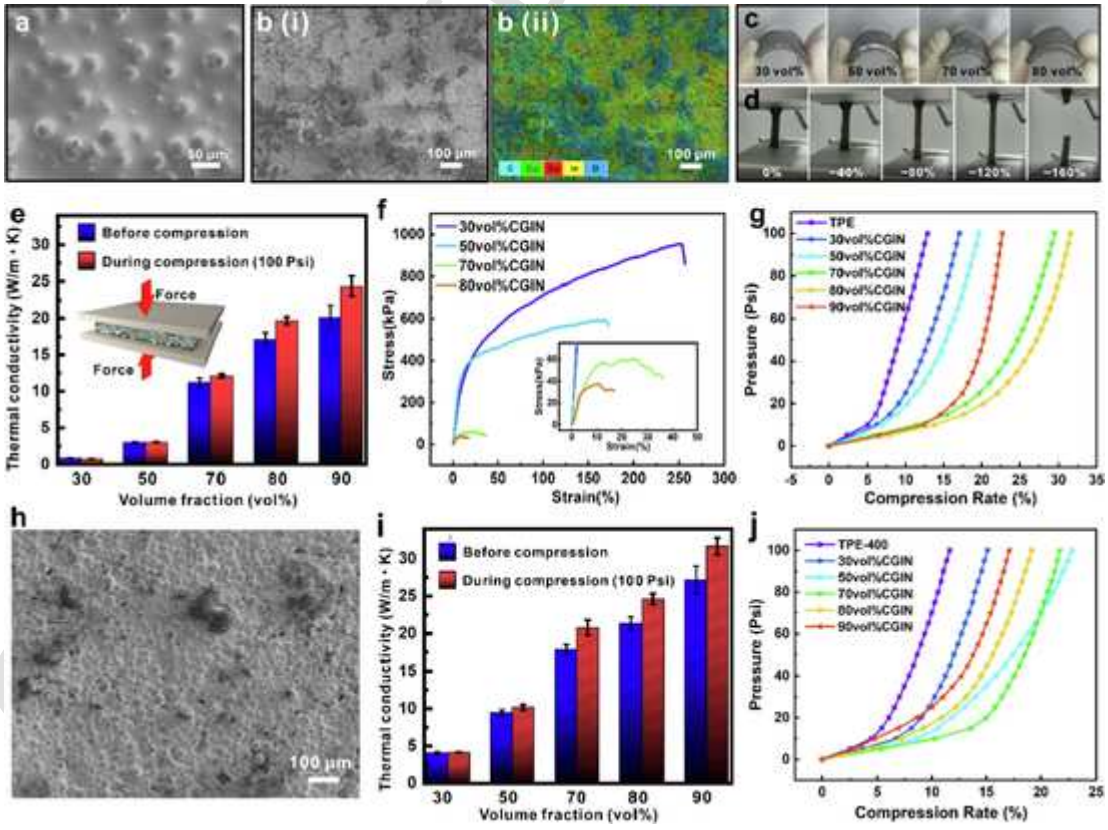

Fig. 4. The SEM images of (a) CPTES modified CuP-EGaIn composite; (b(i)) 80 vol% CGIN/TPE composite and (b(ii)) EDS of carbon, oxygen, copper, gallium and indium in 80 vol% CGIN/TPE composite; Optical photos of (c) 30 vol%, 50 vol%, 70 vol% and 80 vol% CGIN/TPE composites in bending and (d) 50 vol% CGIN/TPE composites in stretching; (e) The thermal conductivities of 30 vol%, 50 vol%, 70 vol%, 80 vol% and 90 vol% CGIN/TPE composites before and during compression (100 Psi); (f) The stress–strain plots of CGIN/TPE composites with different volume ratio of CuP-EGaIn composite; (g) The compression rate plots of pure TPE, CGIN/TPE composites with different volume fraction of CuP-EGaIn composites; (h) SEM image of 80 vol% CGIN/TPE-400 μm; (i) The thermal conductivities of 30 vol%, 50 vol%, 70 vol%, 80 vol% and 90 vol% CGIN/TPE-400 μm composites before and during compression (100 psi); (j) The compression rate plots of pure TPE, CGIN/TPE-400 μm composites with different volume ratio of CuP-EGaIn composites.

measurement system. Compared with pure TPE, the addition of CuP-EGaIn decreases both breaking strain and breaking strength. The reduced stretchability for CGIN/TPE composites is derived from the increasing ratio of paste-like CuP-EGaIn, which has no capacity like polymer matrix of sustaining the external stress. In addition to the stretchability, TIMs are always subjected to certain packaging pressure under actual usage conditions, the ability to be compressed is more important since an excellent compressibility indicates the ease to be deformed to fill the gaps and effectively transport heat across the contact interface. We tested the CGIN/TPE composites under a series of loading pressures and the results are shown in Fig. 4**(g)**. All of the CGIN/TPE composites show enhanced compressibility to some extent compared with pure TPE, and it is reasonable since that the CuP-EGaIn is paste-like and prone to deform when subjected to compression. During the compression, no leakage of liquid metal droplets was observed even we applied a load up to 1.5 MPa (**Figure S10**), which is close to the maximum packaging pressure for TIMs [41]. A stable thermal conductivity is also important in practical uses. It is worth noting that after cycles of bending by hands, the thermal conductivities of 80 vol% CGIN/TPE samples still remain around 17 W/m·K (**Figure S11**). For CGIN/TPE composites, the addition of Cu particles also enhances the electrical conductivity of EGaIn. With the volume fraction of 90%, the CGIN/TPE composite shows an average electrical conductivity of ~ 1.18×10^6 S/m, which is close to the value of pure EGaIn (3.5×10^6 S/m) (Fig. 3**(c)**).

The above results and discussion are based on the composites fabricated by small-sized TPE particles, of which the size is around 100 μm. We further investigated the influence of the TPE particle size on the thermal conductivities of the CGIN/TPE composites by adopting larger-sized TPE particles with the size around 400 μm (TPE-400 μm). As shown in Fig. 4**(h)**, the basic distribution of CuP-EGaIn in CGIN/TPE-400 μm composites is still continuous and presents the continuous distribution as the same with GN/TPE composites and CGIN/TPE composites. We prepared a series of CGIN/TPE-400 μm composites with different volume fractions of CuP-EGaIn and compared the thermal conductivities of the above composites prepared by smaller-sized TPE particles. From Fig. 4**(i)**, the thermal conductivities of composites prepared by larger TPE particles are obviously higher than that of composites prepared by smaller TPE particles (Fig. 4**(e)**) and such difference can be attributed to the different structure caused by the discrepant sizes of TPE particles. During the fabrication of the composites, the mechanical load piles up TPE particles and larger particles leave gaps with larger volume, which are then filled with fluid liquid metal. Therefore, thicker filler network will be formed in the gaps between larger TPE particles. Thicker filler network possesses smaller area of interface between liquid metal and TPE polymer, hence the total internal interface thermal resistance is reduced and the thermal conductivity is enhanced [42–44] At higher pressure, the thermal conductivities of composite fabricated by larger TPE particles behaves similarly as that of composites fabricated by smaller TPE particles (Fig. 4**(e)**). With the same volume fraction of 90%, the CGIN/TPE-400 μm composite under compression possesses the average value of thermal conductivity around 31.69 W/m·K and the highest value ever measured is up to 32.71 W/m·K, a record high in all the polymer-based composites using liquid metal-based fillers as far as we know (Table 1). Fig. 4**(j)** displays compression curves of the CGIN/TPE-400 μm composites. As the similar results with CGIN/TPE composites prepared by smaller-sized TPE particles, the addition of paste-like CuP-EGaIn increases the ability to be compressed compared with pure TPE. As is discussed before, the capacity of being compressed is favored in the packaging of TIMs because it is helpful to fill gaps and decrease contact thermal resistance.

3.4. Thermal management applications

To evaluate the potential application in thermal management, we applied the LM network-based composites as TIMs in a real LED module to test the cross-plane heat dissipation performance, and as a heat spreader to test the in-plane heat spreading performance. The pure TPE and the commercial thermal pad (Laird 780) were used for comparison. The thickness of all the composites in the test was 1 mm. As shown in Fig. 5**(a)**, the composite was placed between a heat sink and a high-power LED chip (10 W). An IR camera monitored the surface temperature of the LED chip. The evaluation of the cross-plane heat dissipation performance was based on the temperature of the LED examined by the IR camera. The higher the cross-plane thermal conductivity, the faster the heat could be transferred out, which would lower the temperature of the LED chips. From Fig. 5**(b)** and Table S4, the average value of the equilibrium temperature of the LED chip was around 92 °C when we used pure TPE as the TIM. After using the commercial thermal pad (Laird 780) as the TIM, the average equilibrium temperature decreased to ~ 52°C. In comparison, the use of the 80 vol% CGIN/TPE composite resulted in the average equilibrium temperature remaining around 41°C, almost half of that of the pure TPE as the TIM. The difference in the heat dissipation among the three samples is visualized vividly in Fig. 5**(c)**, which is detected by an infrared camera. On the other hand, the time for reaching 90% of the equilibrium temperature also reflects the ability of heat conduction. It took about 125 s and 55 s to reach 90% of the equilibrium temperature for the pure TPE and Laird 780, respectively, while the CGIN/TPE composite took less than 15 s. **Figure S12** showed the 80 vol% CGIN/TPE composite as TIMs applied in the

Table 1
Comparison on the in-plane and cross-plane thermal conductivity of the polymer-based composites using LM-based fillers.

Sample	Fabrication method	Filler loading	Average TC (W/m·K)	Year[ref]
GaInSn/methyl silicone oil	Mechanical mixing	81.8%	5.27	2014 [45]
GaInSn/PDMS	Mechanical mixing	66.1%	2.2	2015 [46]
EGaIn/Silicone elastomer	Mechanical mixing; Stretching	50%	4.7 (in-plane) less than 1 (cross-plane)	2017 [2]
Cu-GaInSn/PDMS	Mechanical mixing	50%	10 (frequently 4–8)	2018 [41]
CuP-EGaIn/PDMS	Mechanical mixing	80%	6.7	2018 [10]
Graphene-EGaIn/PDMS	Mechanical mixing	~14 vol%	0.84	2019 [47]
EGaIn/Liquid crystal elastomer	Mechanical mixing	50 vol%	1.70	2019 [3]
Ni-EGaIn/Silicone elastomer	Mechanical mixing; Magnetic alignment	50%	~4 (cross-plane)	2019 [48]
Ga/Silicone elastomer	Sacrificial templating	45%	4.8	2020 [20]
EGaIn/Thermoplastic polymer	Mechanical mixing; Stretching& annealing	70%	11.4 (in-plane)	2020 [15]
Ceramics-GaInSn/Epoxy	Mechanical mixing	50%	2.46	2021 [49]
EGaIn/PDMS foam	Sacrificial templating	15%	0.51 (isotropic) 4.25(in-plane, under 60% compression rate)	2021 [50]
Ag-SiC-GaInSn/silicosis oil	Mechanical mixing	50%	9.9	2021 [51]
GaInSn/aramid nanofiber	Vacuum infiltration	40%	7.14(in-plane) 1.68(cross-plane)	2021 [52]
CuP-EGaIn/Thermoplastic polymer	**Mechanical load under heating**	**70%**	**17.87 (isotropic)**	**This work**
CuP-EGaIn/Thermoplastic polymer	**Mechanical load under heating**	**90%**	**27.18 (isotropic)**	**This work**

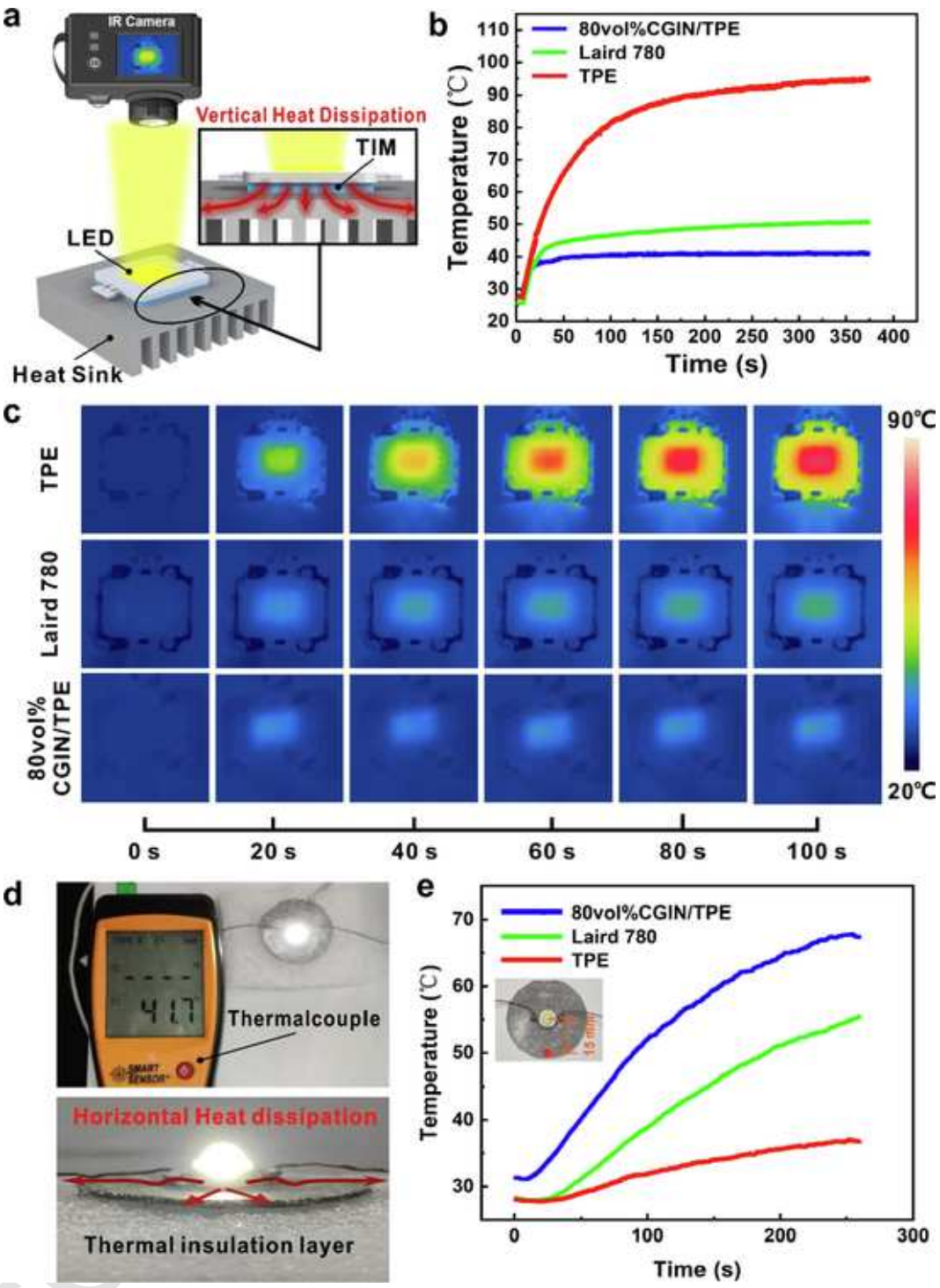

Fig. 5. (a) Schematic of the LED test; (b) The change of the temperature of the LED chip with different TIMs; (c) The infrared images of the LED chip; (d) The setup of the in-plane heat spreading test; (e) The change of the edge temperature of different TIMs. (TPE: thermoplastic elastomer; CGIN/TPE: CuP-EGaIn/thermoplastic elastomer.)

practical thermal management of CPU, indicating its great potential for thermal management. These results indicate that the CGIN/TPE composite possesses promising cross-plane heat dissipation performances for the practical thermal management.

A test on the in-plane heat spreading performance was conducted by using the 80 vol% CGIN/TPE composite as a heat spreader. A LED bulb as a heat source was mounted on the circular samples with diameters of 36 mm, and the edge temperature of the circular samples was recorded by a thermocouple (Fig. 5**(d)**). Heat produced by the LED could only be spread along the plane of the samples because of the thermal insulation from the PU foam under the sample. Fig. 5**(e)** shows that the edge temperature of the CGIN/TPE composite rises faster than the commercial thermal pad and pure TPE. After 260 s, the average value of the edge temperature of the pure TPE, the commercial thermal pad (Laird 780) and the CGIN/TPE composite rise up to 236.7 ℃, 55.4 ℃ and 67.3 ℃, respectively (Table S4). Such measurement confirms the high thermal conductivity in the in-plane direction of the CGIN/TPE composite, and also demonstrates the promising in-plane heat dissipation performance

for the use of the composite as a heat spreader. Additionally, the flexural strength, impact strength, and water-absorbing ability of 80 vol% CGIN/TPE composite used in practical thermal management of this work were also measured shown in Table S5.

For commercial purposes, the cost must be taken into consideration. Table S6 lists the main ingredients of CGIN/TPE composites, and the corresponding unit prices. According to the calculation, the online price of commercially-available thermal pad (Larid 780) is about 3.201 USD/cm^3 while our polymer-based liquid metal composites only costs 1.059 USD/cm^3 (80 vol% CGIN/TPE). The cost of our composites is much lower than the commercial thermal pad (Larid 780). The facile fabrication, the low cost and the obtained high thermal conductivity makes our composites competitive in the field of TIMs.

4. Conclusion

In this work, we established a bottom-up strategy to obtain an isotropic LM network in thermoplastic elastomer, and enhanced the thermal and electrical conductivity of the polymer-based composites for 3D thermal management. The fluidity of LM helps form a percolated 3D network under both the mechanical load and heating. The LM network serves as an effective thermal path for the conduction of heat. The LM network largely enhances the thermal conductivity of the composites in both in-plane and cross-plane directions. The electrical conductivity is also significantly elevated due to the presence of the continuous LM network. The thermal conductivity of 90 vol% CGIN/TPE-400 μm composite can reach as high as 32.71 W/m·K and the electrical conductivity is around 1.18 × 10^6 S/m, close to that of the pure EGaIn, but without the concerns about leakage or smears that occur with pure EGaIn. Meanwhile, the mechanical tests including stretching and compressing both imply good mechanical properties and applicability for practical uses. The investigation on the influence of polymer size on the thermal conductivity where larger polymer particle size will lead to a higher thermal conductivity gives a new insight for tuning the thermal conductivity. Finally, the TIM and heat spreader tests demonstrate the promising performances of heat dissipation of the LM network-based composites in a wide range of practical thermal applications. The approach established in this work provides a simple alternative way for designing and fabricating isotropically and highly thermal and electrical conductive materials, which shows great prospects in future thermal management, flexible electronics, energy conversion and soft robotics.

Declaration of Competing Interest

The authors declare that they have no known competing financial interests or personal relationships that could have appeared to influence the work reported in this paper.

Acknowledgements

Shen Chen and Wenkui Xing contributed equally to this work. The authors are grateful for financial support by National Natural Science Foundation of China (Grant Nos. 51973109, 51521004 and 51873105), the 111 Project (Grant No. B16032), the Innovation Program of Shanghai Municipal Education Commission (Grant No. 2019-01-07-00-02-E00069), and the Center of Hydrogen Science of Shanghai Jiao Tong University. M.D. Dickey is grateful for the support from the National Science Foundation (ASSIST, EEC-1160483 and CMMI-2032409). The authors acknowledge the Instrumental Analysis Center and the Zhiyuan Innovative Research Center of Shanghai Jiao Tong University for providing SEM, Mico-CT, XRD, DSC and LFA analysis.

Appendix A. Supplementary data

Supplementary data to this article can be found online at https://doi.org/10.1016/j.cej.2022.135674.

References

[1] M.R. Khan, C.B. Eaker, E.F. Bowden, M.D. Dickey, Giant and switchable surface activity of liquid metal via surface oxidation, Proc. Natl. Acad. Sci. U. S. A. 111 (39) (2014) 14047–14051.
[2] M.D. Bartlett, N. Kazem, M.J. Powell-Palm, X. Huang, W. Sun, J.A. Malen, C. Majidi, High thermal conductivity in soft elastomers with elongated liquid metal inclusions, Proc. Natl. Acad. Sci. U. S. A. 114 (9) (2017) 2143–2148.
[3] M.J. Ford, C.P. Ambulo, T.A. Kent, E.J. Markvicka, C. Pan, J. Malen, T.H. Ware, C. Majidi, A multifunctional shape-morphing elastomer with liquid metal inclusions, Proc. Natl. Acad. Sci. U. S. A. 116 (43) (2019) 21438–21444.
[4] K. Kalantar-Zadeh, J. Tang, T. Daeneke, A.P. O Mullane, L.A. Stewart, J. Liu, C. Majidi, R.S. Ruoff, P.S. Weiss, M.D. Dickey, Emergence of Liquid Metals in Nanotechnology, ACS Nano 13 (7) (2019) 7388–7395.
[5] N. Kazem, T. Hellebrekers, C. Majidi, Soft Multifunctional Composites and Emulsions with Liquid Metals, Adv. Mater. 29 (27) (2017) 1605985.
[6] A. Zavabeti, J.Z. Ou, B.J. Carey, N. Syed, R. Orrell-Trigg, E.L.H. Mayes, C. Xu, O. Kavehei, A.P. O Mullane, R.B. Kaner, K. Kalantar-zadeh, T. Daeneke, A liquid metal reaction environment for the room-temperature synthesis of atomically thin metal oxides, Science 358 (6361) (2017) 332–335.
[7] S. Chen, Z. Deng, J. Liu, High performance liquid metal thermal interface materials, Nanotechnology 32 (9) (2021) 092001.
[8] R. Tutika, S.H. Zhou, R.E. Napolitano, M.D. Bartlett, Mechanical and Functional Tradeoffs in Multiphase Liquid Metal, Solid Particle Soft Composites, Adv. Funct. Mater. 28 (45) (2018) 1804336.
[9] A. Fassler, C. Majidi, Liquid-phase metal inclusions for a conductive polymer composite, Adv. Mater. 27 (11) (2015) 1928–1932.
[10] P. Fan, Z. Sun, Y. Wang, H. Chang, P. Zhang, S. Yao, C. Lu, W. Rao, J. Liu, Nano liquid metal for the preparation of a thermally conductive and electrically insulating material with high stability, RSC Adv. 8 (29) (2018) 16232–16242.
[11] X. Xu, J. Chen, J. Zhou, B. Li, Thermal Conductivity of Polymers and Their Nanocomposites, Adv. Mater. 30 (17) (2018) e1705544.
[12] G. Yun, S.Y. Tang, S. Sun, D. Yuan, Q. Zhao, L. Deng, S. Yan, H. Du, M.D. Dickey, W. Li, Liquid metal-filled magnetorheological elastomer with positive piezoconductivity, Nat. Commun. 10 (1) (2019) 1300.
[13] Z. Wu, C. Xu, C. Ma, Z. Liu, H.M. Cheng, W. Ren, Synergistic Effect of Aligned Graphene Nanosheets in Graphene Foam for High-Performance Thermally Conductive Composites, Adv. Mater. 31 (19) (2019) e1900199.
[14] W. Dai, L. Lv, T. Ma, X. Wang, J. Ying, Q. Yan, X. Tan, J. Gao, C. Xue, J. Yu, Y. Yao, Q. Wei, R. Sun, Y. Wang, T.H. Liu, T. Chen, R. Xiang, N. Jiang, Q. Xue, C.P. Wong, S. Maruyama, C.T. Lin, Multiscale Structural Modulation of Anisotropic Graphene Framework for Polymer Composites Achieving Highly Efficient Thermal Energy Management, Adv. Sci. 8 (2021) 2003734.
[15] A.B.M.T. Haque, R. Tutika, R.L. Byrum, M.D. Bartlett, Programmable Liquid Metal Microstructures for Multifunctional Soft Thermal Composites, Adv. Funct. Mater. 30 (25) (2020) 2000832.
[16] F. Zhang, Y. Feng, W. Feng, Three-dimensional interconnected networks for thermally conductive polymer composites: Design, preparation, properties, and mechanisms, Mater. Sci. Eng. R Rep. 142 (2020) 100580.
[17] Q.-Q. Bai, X. Wei, J.-H. Yang, N. Zhang, T. Huang, Y. Wang, Z.-W. Zhou, Dispersion and network formation of graphene platelets in polystyrene composites and the resultant conductive properties, Compos. Part A Appl. Sci. Manuf. 96 (2017) 89–98.
[18] A. Kernin, K. Wan, Y. Liu, X. Shi, J. Kong, E. Bilotti, T. Peijs, H. Zhang, The effect of graphene network formation on the electrical, mechanical, and multifunctional properties of graphene/epoxy nanocomposites, Compos. Sci. Technol. 169 (2019) 224–231.
[19] C. Liu, W. Wu, D. Drummer, Y. Wang, Q. Chen, X. Liu, K. Schneider, Significantly enhanced thermal conductivity of polymer composites via establishing double-percolated expanded graphite/multi-layer graphene hybrid filler network, Eur. Polym. J. 160 (2021) 110768.
[20] D. Yu, Y. Liao, Y. Song, S. Wang, H. Wan, Y. Zeng, T. Yin, W. Yang, Z. He, A Super-Stretchable Liquid Metal Foamed Elastomer for Tunable Control of Electromagnetic Waves and Thermal Transport, Adv Sci (Weinh) 7 (12) (2020) 2000177.
[21] X. Wang, P. Wu, Preparation of Highly Thermally Conductive Polymer Composite at Low Filler Content via a Self-Assembly Process between Polystyrene Microspheres and Boron Nitride Nanosheets, ACS Appl. Mater. Interfaces 9 (23) (2017) 19934–19944.
[22] P. Zhang, X. Zhang, X. Ding, Y. Wang, M. Shu, X. Zeng, Y.i. Gong, K. Zheng, X. Tian, Construction of low melting point alloy/graphene three-dimensional continuous thermal conductive pathway for improving in-plane and through-plane thermal conductivity of poly(vinylidene fluoride) composites, Nanotechnology 31 (47) (2020) 475709.
[23] C.P. Feng, L.B. Chen, G.L. Tian, S.S. Wan, L. Bai, R.Y. Bao, Z.Y. Liu, M.B. Yang, W. Yang, Multifunctional Thermal Management Materials with Excellent Heat Dissipation and Generation Capability for Future Electronics, ACS Appl. Mater. Interfaces 11 (20) (2019) 18739–18745.
[24] J. Chen, X. Huang, B. Sun, P. Jiang, Highly Thermally Conductive Yet Electrically

Insulating Polymer/Boron Nitride Nanosheets Nanocomposite Films for Improved Thermal Management Capability, ACS Nano 13 (1) (2019) 337–345.
[25] N. Kränzlin, M. Niederberger, Controlled fabrication of porous metals from the nanometer to the macroscopic scale, Mater. Horizons 2 (4) (2015) 359–377.
[26] B. Yao, W. Hong, T. Chen, Z. Han, X. Xu, R. Hu, J. Hao, C. Li, H. Li, S.E. Perini, M.T. Lanagan, S. Zhang, Q. Wang, H. Wang, Highly Stretchable Polymer Composite with Strain-Enhanced Electromagnetic Interference Shielding Effectiveness, Adv. Mater. 32 (14) (2020) e1907499.
[27] Y. Huang, B. Yu, L. Zhang, N. Ning, M. Tian, Highly Stretchable Conductor by Self-Assembling and Mechanical Sintering of a 2D Liquid Metal on a 3D Polydopamine-Modified Polyurethane Sponge, ACS Appl. Mater. Interfaces 11 (51) (2019) 48321–48330.
[28] J. Tang, X. Zhao, J. Li, R. Guo, Y. Zhou, J. Liu, Gallium-Based Liquid Metal Amalgams: Transitional-State Metallic Mixtures (TransM(2)ixes) with Enhanced and Tunable Electrical, Thermal, and Mechanical Properties, ACS Appl. Mater. Interfaces 9 (41) (2017) 35977–35987.
[29] R.W. Style, R. Tutika, J.Y. Kim, M.D. Bartlett, Solid-Liquid Composites for Soft Multifunctional Materials, Adv. Funct. Mater. 31 (1) (2020) 2005804.
[30] Y. Lin, C. Cooper, M. Wang, J.J. Adams, J. Genzer, M.D. Dickey, Handwritten, Soft Circuit Boards and Antennas Using Liquid Metal Nanoparticles, Small 11 (48) (2015) 6397–6403.
[31] Y. Lin, J. Genzer, M.D. Dickey, Attributes, Fabrication, and Applications of Gallium-Based Liquid Metal Particles, Adv Sci (Weinh) 7 (12) (2020) 2000192.
[32] H. Wang, W. Xing, S. Chen, C. Song, M.D. Dickey, T. Deng, Liquid Metal Composites with Enhanced Thermal Conductivity and Stability Using Molecular Thermal Linker, Adv Mater 33 (43) (2021) 2103104.
[33] W. Kong, Z. Wang, M. Wang, K.C. Manning, A. Uppal, M.D. Green, R.Y. Wang, K. Rykaczewski, Oxide-Mediated Formation of Chemically Stable Tungsten-Liquid Metal Mixtures for Enhanced Thermal Interfaces, Adv. Mater. 31 (44) (2019) e1904309.
[34] H. Yuan, Y. Wang, T. Li, Y. Wang, P. Ma, H. Zhang, W. Yang, M. Chen, W. Dong, Fabrication of thermally conductive and electrically insulating polymer composites with isotropic thermal conductivity by constructing a three-dimensional interconnected network, Nanoscale 11 (23) (2019) 11360–11368.
[35] J. Chen, X. Huang, Y. Zhu, P. Jiang, Cellulose Nanofiber Supported 3D Interconnected BN Nanosheets for Epoxy Nanocomposites with Ultrahigh Thermal Management Capability, Adv. Funct. Mater. 27 (5) (2017) 1604754.
[36] F. Wu, S. Chen, X. Tang, H. Fang, H. Tian, D. Li, X. Peng, Thermal conductivity of polycaprolactone/three-dimensional hexagonal boron nitride composites and multi-orientation model investigation, Compos. Sci. Technol. 197 (2020) 108245.
[37] Y. Agari, T. u., Estimation on Thermal Conductivities of Filled Polymers, J. Appl. Polym. Sci. 32 (7) (1986) 5705–5712.
[38] S. Yang, W. Li, S. Bai, Q. Wang, Fabrication of Morphologically Controlled Composites with High Thermal Conductivity and Dielectric Performance from Aluminum Nanoflake and Recycled Plastic Package, ACS Appl. Mater. Interfaces 11 (3) (2019) 3388–3399.
[39] P. Zhang, P. Yuan, X. Jiang, S. Zhai, J. Zeng, Y. Xian, H. Qin, D. Yang, A Theoretical Review on Interfacial Thermal Transport at the Nanoscale, Small 14 (2) (2018) 1702769.
[40] H. Charaya, T.G. La, J. Rieger, H.J. Chung, Thermochromic and Piezocapacitive Flexible Sensor Array by Combining Composite Elastomer Dielectrics and Transparent Ionic Hydrogel Electrodes, Adv. Mater. Technol. 4 (9) (2019) 1900327.
[41] M.I. Ralphs, N. Kemme, P.B. Vartak, E. Joseph, S. Tipnis, S. Turnage, K.N. Solanki, R.Y. Wang, K. Rykaczewski, In Situ Alloying of Thermally Conductive Polymer Composites by Combining Liquid and Solid Metal Microadditives, ACS Appl. Mater. Interfaces 10 (2) (2018) 2083–2092.
[42] H. Chen, V.V. Ginzburg, J. Yang, Y. Yang, W. Liu, Y. Huang, L. Du, B. Chen, Thermal conductivity of polymer-based composites: Fundamentals and applications, Prog. Polym. Sci. 59 (2016) 41–85.
[43] Y. Wang, J. Wu, Y. Yin, T. Han, Effect of micro and nano-size boron nitride and silicon carbide on thermal properties and partial discharge resistance of silicone elastomer composite, IEEE T. Dielect. El. In. 27 (2) (2020) 377–385.
[44] H. He, R. Fu, Y. Han, Y. Shen, D. Wang, High Thermal Conductive Si3N4 Particle Filled Epoxy Composites With a Novel Structure, J. Electron. Packaging 129 (4) (2007) 469–472.
[45] S. Mei, Y. Gao, Z. Deng, J. Liu, Thermally Conductive and Highly Electrically Resistive Grease Through Homogeneously Dispersing Liquid Metal Droplets Inside Methyl Silicone Oil, J. Electron. Packaging 136 (1) (2014) 011009.
[46] S.H. Jeong, S. Chen, J. Huo, E.K. Gamstedt, J. Liu, S.L. Zhang, Z.B. Zhang, K. Hjort, Z. Wu, Mechanically Stretchable and Electrically Insulating Thermal Elastomer Composite by Liquid Alloy Droplet Embedment, Sci Rep 5 (2015) 18257.
[47] Y. Sargolzaeiaval, V.P. Ramesh, T.V. Neumann, R. Miles, M.D. Dickey, M.C. Öztürk, High Thermal Conductivity Silicone Elastomer Doped with Graphene Nanoplatelets and Eutectic GaIn Liquid Metal Alloy, ECS J. Solid State Sc. 8 (6) (2019) P357–P362.
[48] M. Ralphs, W. Kong, R.Y. Wang, K. Rykaczewski, Thermal Conductivity Enhancement of Soft Polymer Composites through Magnetically Induced Percolation and Particle-Particle Contact Engineering, Adv. Mater. Interfaces 6 (6) (2019) 1801857.
[49] S.-W. Xiong, P. Zhang, Q. Zou, Y. Xia, M.-Y. Jiang, J.-G. Gai, High thermal conductivity and electrical insulation of liquid alloy/ceramic/epoxy composites through the construction of mutually independent structures, Compos. Sci. Technol. 202 (2021) 108596.
[50] B. Yao, X. Xu, H. Li, Z. Han, J. Hao, G. Yang, Z. Xie, Y. Chen, W. Liu, Q. Wang, H. Wang, Soft liquid-metal/elastomer foam with compression-adjustable thermal conductivity and electromagnetic interference shielding, Chem. Eng. J. 410 (2021) 128288.
[51] W. Kong, Z. Wang, N. Casey, M.M. Korah, A. Uppal, M.D. Green, K. Rykaczewski, R.Y. Wang, High Thermal Conductivity in Multiphase Liquid Metal and Silicon Carbide Soft Composites, Adv. Mater. Interfaces 8 (14) (2021) 2100069.
[52] L.-C. Jia, Y.-F. Jin, J.-W. Ren, L.-H. Zhao, D.-X. Yan, Z.-M. Li, Highly thermally conductive liquid metal-based composites with superior thermostability for thermal management, J. Mater. Chem. C 9 (8) (2021) 2904–2911.